APPENDIX C

"Single-Molecule Reader for High-Throughput Bioanalysis" by Hesse, *et al.*, Anal.Chem. 76 (2004):5960-5964

Anal. Chem. **2004**, *76*, 5960–5964

Technical Notes

Single-Molecule Reader for High-Throughput Bioanalysis

Jan Hesse,[†] Max Sonnleitner,[‡] Alois Sonnleitner,[‡] Günter Freudenthaler,[‡] Jaroslaw Jacak,[†] Otmar Höglinger,[‡] Hansgeorg Schindler,[†,‡] and Gerhard J. Schütz*[,†]

Biophysics Institute, Johannes-Kepler-University Linz, Altenbergerstrasse 69, A-4040 Linz, Austria, and Center for Biomedical Nanotechnology, Upper Austrian Research GmbH, Scharitzerstrasse 6-8, A-4020 Linz, Austria

We report here the development of a device for single-molecule imaging on large surface areas. A CCD camera operated in time delay and integration mode is synchronized with the movement of a sample scanning stage, enabling continuous data acquisition. Experiments on single fluorescent lipid molecules in supported lipid bilayers and on stained living cells demonstrate the capabilities of the method. Areas of up to 5 × 5 mm^2 were recorded within 11 min at a pixel size of 129 nm.

Analytical investigation of biological material is a challenge to the sensitivity of any detection device. An individual cell contains a total amount of ~10^6 protein molecules. While the most abundant proteins can be expressed with up to 10^5 copies, highly relevant minor populations often occur at an expression level of only a few hundred molecules per cell. Mass spectrometry[1-3] and capillary electrophoresis[4] have become methods of choice for sensitive protein analysis. However, no bioanalytical method is currently capable of determining minor protein populations in single cells. Fluorescence has proven to be one of the most sensitive measurands in bioanalytics. Recently, fluorescence microscopy has been established as a tool to detect trace amounts of analyte in various environments, even at the level of single molecules.[5-11] Although fluorescence-based detection systems are heavily used for proteomics and genomics research,[12-14] no single-molecule detection device for chip readout has been reported. Here we provide the conceptual basis for ultrasensitive proteomics and genomics by reporting the design of a chip reader, which operates at diffraction-limited resolution and single-molecule sensitivity. The device is capable of imaging areas of 5 × 5 mm within 11 min.

To ensure flexibility, the reader has been set up on a conventional inverted epifluorescence microscope (Zeiss). Samples were mounted on a high-precision scanning stage (Märzhäuser) and illuminated through the epiport of the microscope by 633-nm laser light from a dye laser (Spectra Physics) (Figure 1). Fluorescence signals were collected using a 100× oil immersion objective (Zeiss Plan Neofluar, NA = 1.3) and imaged on a back-illuminated NTE/CCD camera (QE, ≥85%; chip size, C = 1300 pixels in serial and L = 100 pixels in parallel direction; pixel size, 20 μm; Roper Scientific). Apertures in the baseport of the fluorescence microscope limit the field of view to C = 1000 pixels in serial direction. Residual Rayleigh and Raman scattered light was effectively blocked using appropriate filter combinations (Chroma).

Conventional microscope-based scanning systems acquire sequential images in order to cover large areas. The time T_{seq} required for recording a given sample area A can be calculated according to

$$T_{seq} = \frac{A}{\delta^2}\left[t_{readout} + \frac{t_{line-shift}}{C} + \frac{t_{ill} + t_{positioning}}{LC}\right] \quad (1)$$

with δ the pixel size in the object plane. The sum represents contributions of the illumination time t_{ill}, the time to digitize each pixel $t_{readout}$, the time to shift one line into the readout register $t_{line-shift}$, and additional terms accounting for positioning the stage,

* To whom correspondence should be addressed. Tel.: +43-732-2468-9284. Fax.: +43-732-2468-9280. E-mail: gerhard.schuetz@jku.at.
[†] Johannes-Kepler-University Linz.
[‡] Upper Austrian Research GmbH.

(1) Aebersold, R.; Mann, M. *Nature* **2003**, *422*, 198–207.
(2) Gerber, S. A.; Rush, J.; Stemman, O.; Kirschner, M. W.; Gygi, S. P. *Proc. Natl. Acad. Sci. U.S.A.* **2003**, *100*, 6940–6945.
(3) Li, L.; Garden, R. W.; Sweedler, J. V. *Trends Biotechnol.* **2000**, *18*, 151–160.
(4) Krylov, S. N.; Dovichi, N. J. *Electrophoresis* **2000**, *21*, 767–773.
(5) Shera, E. B.; Seitzinger, N. K.; Davis, L. M.; Keller, R. A.; Soper, S. A. *Chem. Phys. Lett.* **1990**, *174*, 553–557.
(6) Sase, I.; Miyata, H.; Corrie, J. E.; Craik, J. S.; Kinosita, K., Jr. *Biophys. J.* **1995**, *69*, 323–328.
(7) Funatsu, T.; Harada, Y.; Tokunaga, M.; Saito, K.; Yanagida, T. *Nature* **1995**, *374*, 555–559.
(8) Schmidt, T.; Schutz, G. J.; Baumgartner, W.; Gruber, H. J.; Schindler, H. *Proc. Natl. Acad. Sci. U.S.A.* **1996**, *93*, 2926–2929.
(9) Sako, Y.; Minoghchi, S.; Yanagida, T. *Nat. Cell Biol.* **2000**, *2*, 168–172.
(10) Schutz, G. J.; Kada, G.; Pastushenko, V. P.; Schindler, H. *Embo J.* **2000**, *19*, 892–901.
(11) Schutz, G. J.; Pastushenko, V. P.; Gruber, H. J.; Knaus, H.-G.; Pragl, B.; Schindler, H. *Single Mol.* **2000**, *1*, 25–31.
(12) Zhu, H.; Bilgin, M.; Bangham, R.; Hall, D.; Casamayor, A.; Bertone, P.; Lan, N.; Jansen, R.; Bidlingmaier, S.; Houfek, T.; Mitchell, T.; Miller, P.; Dean, R. A.; Gerstein, M.; Snyder, M. *Science* **2001**, *293*, 2101–2105.
(13) MacBeath, G.; Schreiber, S. L. *Science* **2000**, *289*, 1760–1763.
(14) Pawlak, M.; Schick, E.; Bopp, M. A.; Schneider, M. J.; Oroszlan, P.; Ehrat, M. *Proteomics* **2002**, *2*, 383–393.

10.1021/ac049300f CCC: $27.50
Published on Web 09/03/2004

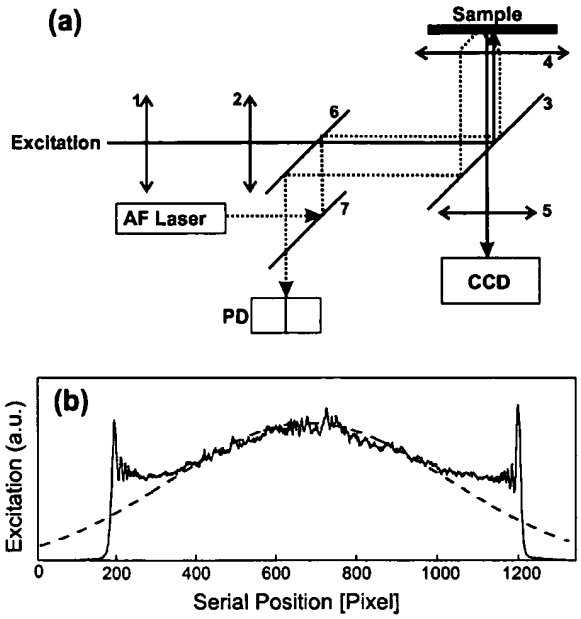

Figure 1. (a) Scheme of the apparatus. The 633-nm excitation light passes through a laser beam line generator (1) and a 80-mm spherical lens (2). It is reflected on a dichroic beam splitter (3) and focused via the objective (4) onto the sample. Fluorescence emission is collected throught the same objective and imaged via the tube lens (5) onto the camera chip. For the focus-hold system, the autofocus (AF) laser is overlaid with the excitation beam using a dichroic beam splitter (6). Back-reflected light is separated on a 50% beam splitter (7) and imaged on a two-segment photodiode. (b) Cross section of the excitation profile perpendicular to the scanning direction (solid line). The sharp edges are mandatory for proper illumination (photobleaching). For comparison, a Gaussian function (dashed line) is shown which fits the central region of the excitation profile.

subsumed in $t_{positioning}$; L gives the total number of lines on the chip. Frame-transfer cameras acquire signals during the readout process, which allows neglecting t_{ill} in eq 1. However, proper sample positioning limits the overall readout speed in any sequential recording device. There, inertia of the moving parts requires time-consuming feedback loops for precise stops. For example, sample shift by 20 μm with a precision according to the pixel size of 200 nm in the object plane takes about 0.2–2 s, depending on the motorized sample stage. Assuming the parameter used in this study (a digitization rate of 1 MHz, $t_{line-shift} = 12$ μs and $\delta = 0.2$ μm), a rectangular stripe with a size of 1 × 0.02 cm^2 can be imaged within 2.5–17.5 min.

Here we present a scanning system that avoids overhead times due to both stage positioning and illumination, based on the implementation of synchronized continuous stage-shift and camera readout.[15] For this, the camera is operated in time delay and integration (TDI) mode, a mode developed for astronomy to acquire long swaths of moving objects, especially at low light levels.[16-19] In this mode, the parallel register shift is synchronized with the object motion, so that charge packets on the CCD pixels always correspond to the same image region as they move across the parallel register. Charge accumulates and signal strength increases as the pixels approach the readout register. For application of the TDI mode to microscopy, we synchronized image and sample shift by running the camera as master, which provided trigger signals to the scanning stage upon each line shift. TDI-based scanning allows reaching the theoretical minimum for the scanning time of

$$T_{TDI} = \frac{A}{\delta^2}\left[\frac{t_{line-shift}}{C} + t_{readout}\right] \qquad (2)$$

Continuous readout enables the acquisition of images larger than the CCD chip size in parallel direction, only limited by the storage capacity of the computer. In such a configuration, signal integration time is equal to $LCt_{readout} + Lt_{line-shift}$. In general, the field of excitation can be chosen arbitrarily. However, too large excitation areas lead to photobleaching of parts of the sample outside of the detection area. In contrast, too small excitation areas might result in saturation of the fluorescence signal due to the increased excitation intensity.[20] For wide-field illumination, we chose here a Gaussian profile with a full width at half-maximum (fwhm) of ~50 pixels (corresponding to 10 μm in the object plane) in the parallel direction. For a CCD chip size of 100 pixels, this configuration ensures that 98% of the excitation light is imaged onto the detection area. Defocusing of the excitation beam in the object plane was achieved by inserting a spherical lens with a focal length of 80 mm in the illumination path.

To allow comparison between TDI mode and conventional imaging, we define here an effective illumination time, $\hat{t}_{ill}$. Given a signal recorded in TDI mode, $\hat{t}_{ill}$ represents the illumination equivalent for detecting the same signal in conventional imaging. If $n_{seq} = \omega I_{max} t_{ill}$ represents the number of excitation cycles in a homogeneous excitation beam profile of intensity I_{max},[21] and $n_{TDI} = \omega \int I(x)\, dt$ the number of excitation cycles in TDI mode, $\hat{t}_{ill}$ is defined as the time for which n_{seq} equals n_{TDI}; i.e., $n_{seq}(\hat{t}_{ill}) = n_{TDI}$. Assuming a Gaussian beam profile with $I(x) = I_{max} \exp[-x^2/2\sigma^2]$ in parallel direction, the effective illumination time is given by $\hat{t}_{ill} = (2\pi)^{1/2}\sigma[Ct_{readout} + t_{line-shift}]$. For the camera used in this study, $\hat{t}_{ill}$ equals 53 ms. The total recording time in TDI mode for a 1 × 0.02 cm stripe is 50 s (eq 2), assuming the same system settings as in conventional imaging mode.

In the serial direction, it is again necessary to restrict the excitation light to the detection area in order to reduce photobleaching. In addition, a homogeneous excitation profile is now crucial for quantitative imaging. A possible way to achieve these constraints would be to image a homogeneously illuminated rectangular mask onto the sample. The loss of illumination light at the mask, however, requires high laser power to ensure excitation intensities of ~kW/cm^2, as needed for single-molecule detection. A proper way to fully utilize the available laser power is the use of an aspherical lens for defocusing the laser beam

(15) Schindler, H. In PCT/AT99/00257; Schindler, H. international patent, 2000.
(16) McGraw, J. T.; Angel, J. R. P.; Sargent, T. A. In *Applications of Digital Image Processing to Astronomy*; Eliot, D. A., Ed.; SPIE: Bellingham, MA, 1980; Vol. 264, p 20.
(17) Dereniak, E. L.; Crowe, D. G. *Optical Radiation Detectors*; Wiley: New York, 1984.
(18) Gibson, B. K.; Hickson, P. *Mon. Not. R. Astron. Soc.* **1992**, *258*, 543–551.
(19) Sajan, M. R.; Tay, C. J.; Shang, H. M.; Asundi, A. *Opt. Laser Technol.* **1997**, *29*, 327–331.
(20) Schmidt, T.; Schutz, G. J.; Baumgartner, W.; Gruber, H. J.; Schindler, H. *J. Phys. Chem.* **1995**, *99*, 17662–17668.
(21) Demtröder, W. *Laser Spectroscopy*; Springer: Heidelberg, 1996.

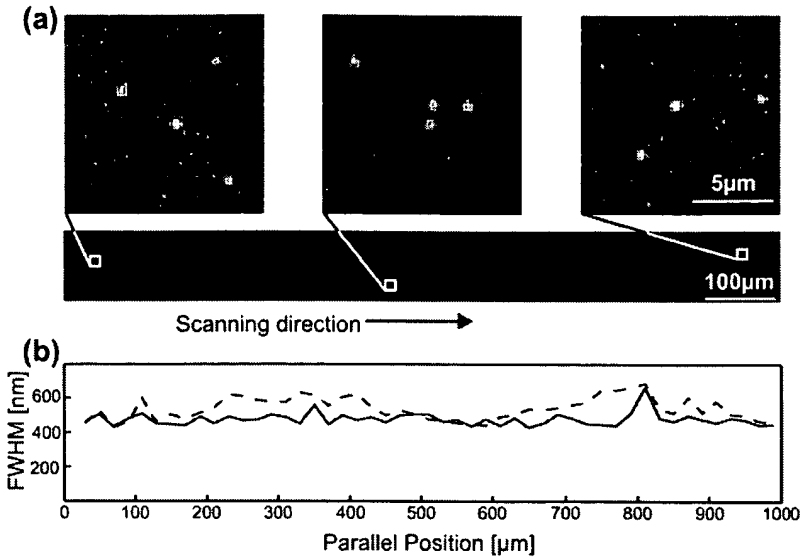

Figure 2. (a) Image of a supported lipid bilayer (DPPC) containing trace amounts of fluorescent lipid (Cy5-DPPE/DPPC, 10^{-8} molar ratio). The stripe shows a 1 × 0.1 mm^2 region of the bilayer; arbitrarily chosen details demonstrate the homogeneity of the bilayer over the full scanning region. Individual fluorescent peaks can be easily discriminated over background and represent individual Cy5-DPPE molecules. (b) Variation of the width of the point spread function in scanning direction, measured from 1350 single molecules. For this, the image was divided into subregions of 100 × 20 μm^2, and the average signal width was determined by fitting an elliptical Gaussian profile to each single-molecule signal. The solid line corresponds to the short axis of the signal profile, which is oriented perpendicular to the scanning direction. The average value of 450 nm compares well with the diffraction-limited spot size. In scanning direction, peaks are slightly broadened due to the combination of continuous and discrete shifting procedures (dashed line).

along the serial direction. For this, a commercial laser beam line generator (Powell lens, Oz Optics) with a divergence of 5° (half-angle) has been placed 13 cm before the spherical lens into the excitation path. In combination with the objective lens, this yields an excitation profile in serial direction with a fwhm of ~1000 pixels, which sharply declines to zero at the edges (Figure 1b). This shape is preferential compared to a Gaussian profile, indicated in the figure by a dashed line. For quantitative imaging, residual inhomogeneities of the excitation profile have been corrected.

Repeated scanning of neighboring stripes allows covering arbitrary sizes of the sample. However, thickness variations of the glass coverslip or slight tilt angles of the mounted sample lead to significant defocusing of several micrometers during the scanning process. To ensure proper focusing over the whole image, an automatic focus-hold system has been employed.[22] For this, a second laser (frequency-doubled Nd:YAG with a wavelength of 532 nm, Spectra Physics) with a power of 1 mW was overlaid with the illumination beam and imaged onto the sample next to the detection area. Upon reflection on the upper glass surface, the beam was recollimated through the objective. Changes in the distance between the surface of the coverslip and the objective result in changes in the angle of the out-coupled beam, which are detected on a two-segment photodiode (Hamamatsu). The differential signal was used as input into a PID controller operated in feedback loop; the output of this controller was connected to a piezodriven focusing system (Physik Instrumente).

To demonstrate proof of principles, the device was applied to image a supported lipid bilayer on a glass coverslip, containing trace amounts of fluorescent-labeled lipid (Figure 2). The bilayer was formed by vesicle fusion.[23] Briefly, a 2.5 mg/mL vesicle solution of dipalmitoylphosphatidycholine (DPPC, Avanti Polar Lipids) containing a molar fraction of 10^{-8} Cy5-labeled dipalmitoylphosphatidylethanolamine (Cy5-DPPE[10]) was prepared in phosphate-buffered saline (PBS). At room temperature, this lipid forms a bilayer in gel phase; the DPPC matrix is characterized by a lateral diffusion constant of $D_{lat} \sim 10^{-12}$ cm^2/s,[24] which allows one to treat individual Cy5-DPPE molecules as immobilized on the length and time scale of the experiment. A 10-μL sample of the vesicle solution was deposited onto the coverslip, incubated for 30 min, and finally diluted with 1 mL of pure PBS. Figure 2a shows a 1 × 0.1 mm image of the bilayer, recorded in TDI mode. It appears homogeneous, containing randomly distributed fluorescence peaks of Cy5-DPPE, as expected from previous studies on similar systems.[25,26] The observed surface density of ~1.4 Cy5-DPPE molecules/100 μm^2 is in good agreement with the theoretical prediction of 2.1 molecules/100 μm^2, assuming a mean area of 48 Å^2/DPPC molecule.[27] The total counts emitted by individual dye molecules were analyzed by fitting a two-dimensional Gaussian function,[8] yielding a median of $F \sim 812$ counts (Figure 3). Taking into account the illumination time $\hat{t}_{ill} = 53$ ms and the excitation intensity of $I_{max} = 0.5$ kW/cm^2, this value compares well with previous measurements on single Cy5-labeled lipids.[10] Due to the high signal amplitude, individual fluorescence peaks could be

(22) Hellen, E. H.; Axelrod, D. *Rev. Sci. Instrum.* **1990**, *61*, 3722.

(23) Kalb, E.; Frey, S.; Tamm, L. K. *Biochim. Biophys. Acta* **1992**, *1103*, 307–316.
(24) Tamm, L. K.; McConnell, H. M. *Biophys. J.* **1985**, *47*, 105–113.
(25) Harms, G. S.; Sonnleitner, M.; Schutz, G. J.; Gruber, H. J.; Schmidt, T. *Biophys. J.* **1999**, *77*, 2864–2870.
(26) Schutz, G. J.; Schindler, H.; Schmidt, T. *Biophys. J.* **1997**, *73*, 1073–1080.
(27) Sun, W.; Suter, R. M.; Knewtson, M. A.; Worthington, C. R.; Tristram-Nagle, S.; Zhang, R.; Nagle, J. F. *Phys. Rev.. E* **1994**, *49*, 4665–4676.

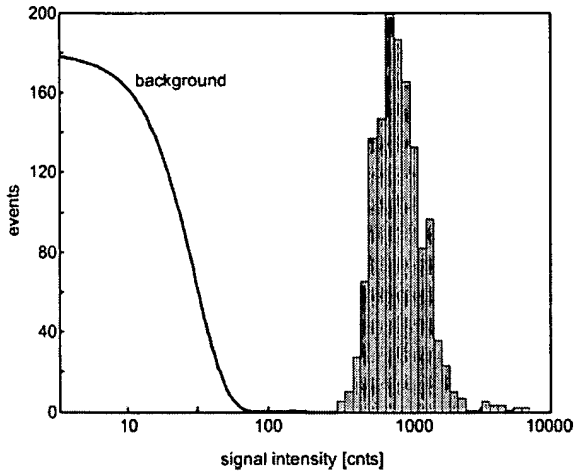

Figure 3. Histogram of the single-molecule signal intensity recorded on the bilayer shown in Figure 2, plotted in logarithmic scale. The signals clearly exceed the background, yielding a mean signal to background noise ratio of ~37. This allows one to unambiguously detect basically all dye molecules on the glass slide. To improve visibility, distribution of the background signal has been plotted as a probability density function.

easily discriminated against the background noise of 10 counts rms per pixel, which corresponds to 22 counts per diffraction-limited spot. The mean signal to background noise ratio for single-molecule detection is therefore given by a value of ~37. The high discrimination certainty allows one to unambiguously detect basically all fluorescent molecules on the glass surface.

The point spread function for the imaging system has been characterized on 30-nm Cy5-labeled polystyrene beads, yielding a fwhm of 470 nm in the focal plane.[11] For the combination of discrete (camera line-shift) and continuous (scanning stage) shifting procedures used in this study, an additional widening of the point spread function of ~12% in scanning direction is expected. Analysis of 1350 peaks with an elliptical two-dimensional Gaussian function yielded an average $\text{fwhm}_1 = 510$ nm in scanning direction and $\text{fwhm}_2 = 450$ nm in the perpendicular direction. Importantly, both values show no significant variation over the scan, demonstrating the proper function of the focus-hold system (Figure 2b). The average peak distortion of 13% for this scan indicates optimum synchronization of camera line-shift and stage movement.

Assembly of individual stripes to one high-resolution image demands for reproducibility of the scanning process. Comparison of the positions of individual Cy5-DPPE molecules on repeated scans of the same area revealed minor fluctuations with a standard deviation of 100 nm (37 nm) in (perpendicular to) the scanning direction. The second value is close to the positional accuracy of the Gaussian fit[26] and indicates only slight deviations from a perfectly linear scan. The first value is larger and may be caused by velocity changes of the sample stage due to residual irregularities in the spindle slope. It should be noted that both values are below the diffraction limit of the imaging process.

The coverslip may also be loaded with living cells for in vivo protein expression profiling. Figure 4 shows an example of adherent HEP2 cells growing on a fibronectin-coated glass slide. The cells were stained with MitoTracker Deep Red 633 (Molecular Probes), a specific label for mitochondria. Staining was very

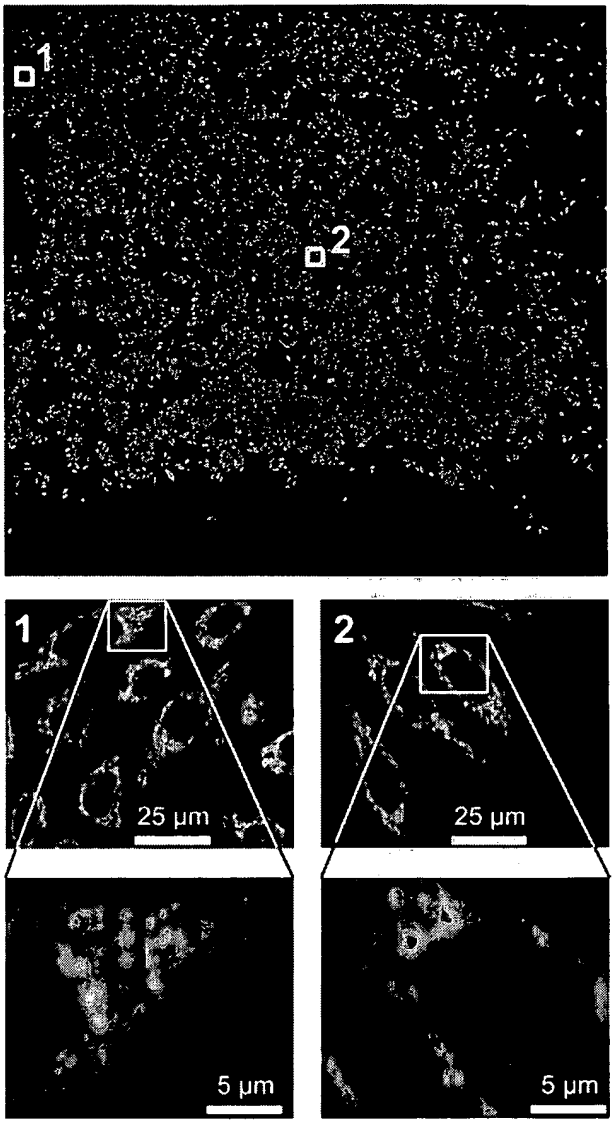

Figure 4. Large scan of live HEP2 cells stained with MitoTracker Deep Red 633 to visualize mitochondria. The 5 × 5 mm^2 image was recorded within 11 min at a pixel size of 129 nm in the image plane. The details show nicely the typical pattern of mitochondrial organization in the cytoplasm of the cells. Residual movements of cells during the recording process can lead to slight mismatches of adjacent stripes (e.g., magnification of detail 1).

efficient and resulted in signals much stronger than signals obtained from single dye molecules; therefore, we reduced the laser power to ~30 W/cm^2. To achieve high-speed imaging, which is crucial for live cell observations, the image was recorded on a fast CCD camera (Cool Snap HQ, 10 MHz, $C = 1392$ pixels in serial and $L = 1040$ pixels in parallel direction, pixel size 6.45 µm; Roper Scientific). Using a 100× objective and symmetric binning of two, a pixel size of 129 nm in the object plane was obtained. The quantum efficiency of this camera of ~60% still allows for single-molecule observations, however, at reduced signal-to-noise ratio (data not shown).

The fast camera enabled readout times down to 300 µs/line. Due to the larger chip size, the illumination time $\hat{t}_{\text{ill}}$ increased to

106 ms. Figure 4 shows a 5 × 5 mm^2 area of the sample (corresponding to 1.5 G pixels), which consists of 56 stripes with a width of 90 μm. Each stripe was recorded within 11.6 s, yielding an overall acquisition time of ~11 min. Individual cells can be easily discriminated, showing the characteristic distribution of mitochondria over the cytoplasm. Since the cells were alive during the imaging process, residual motion of individual cells cannot be excluded. This lead to slight misalignments or distortions of the images of cells protruding over two adjacent stripes.

The high acquisition speed obtained here allows one to maintain viability of the cells for the whole scan, making this method a powerful tool for fast prescreening of large populations. Subsequent image processing allows selecting cells of interest, which can then be automatically moved into the observation area and imaged on a faster time scale down to milliseconds. The presented approach can be generalized to multiparameter analysis either by consecutive scanning in different colors or by adding a second detection path. While the first approach is restricted to fixed samples, the latter is also applicable to live cell imaging.

ACKNOWLEDGMENT

This study was supported by the Austrian Federal Ministry of Education, Science and Culture, by the Austrian Research Funds (Project P15057), and by the state of Upper Austria.

Received for review May 12, 2004. Accepted July 12, 2004.

AC049300F